

Accurate Circuit and Device Equations for Designing 50-600 GHz GaAs Schottky Diode Varactor Frequency Doublers

R. E. Lipsey, S. H. Jones, and T. W. Crowe

Department of Electrical Engineering, University of Virginia, Charlottesville, VA 22903

Abstract

The use of GaAs Schottky barrier varactors (SBVs) for high frequency multiplication has long been established. In order to theoretically analyze the performance of these devices, several different approaches have been realized among which are equivalent circuit modeling, drift-diffusion modeling, and Monte Carlo modeling. Equivalent circuit modeling, such as the analytical models derived by Penfield and Rafuse, offer a fast and efficient method for analyzing these non-linear devices. However, the solutions of these analytical models rely heavily on undetermined coefficients. In an attempt to solve the problems associated with the Penfield and Rafuse technique, Burckhardt empirically solved for the undetermined coefficients, creating closed form expressions. These analytical models have demonstrated reasonable accuracy for SBVs in the frequency range of 1-50 GHz. However, at high frequencies, the usefulness of these analytical models is limited due to their inability to model high frequency electron transport phenomenon. To accurately model high frequency transport phenomena in GaAs SBVs, a Monte Carlo Harmonic-Balance (MCHB) simulator has been developed and offers considerably better precision over results obtained from Harmonic-Balance simulation incorporating equivalent circuit modeling for the diodes. Although the MCHB and DDHB methods offer superior accuracy, they are time and CPU intensive and can take from several hours to several weeks to reach a complete multiplier design. To decrease simulation complexity and maintain precision, we have derived a set of analytical design equations with semi-empirical coefficients derived from the MCHB simulator. Since these expressions for device and circuit impedance, efficiency, output power, and d.c. bias are independent of each other and rely solely on nominal device specifications, they allow for co-design from both a device and circuit point of view in a relatively simple, efficient, and accurate manner. Results from the set of design equations are compared to both MCHB simulations and experimental results for the UVA 5T1 100 to 200 GHz frequency doubler.

I. Introduction

The use of GaAs Schottky barrier varactors (SBVs) for high frequency multiplication has long been established. In order to theoretically analyze the performance of these devices, several different approaches have been realized among which are equivalent circuit modeling, drift-diffusion modeling, and Monte Carlo modeling. Equivalent circuit modeling, such as the analytical models derived by Penfield and Rafuse [1], offer a fast and efficient method for analyzing these non-linear devices. However, the solutions of these analytical models rely heavily on undetermined coefficients. In an attempt to solve the problems associated with the Penfield and Rafuse technique, Burckhardt [2] empirically solved for the undetermined coefficients, creating closed form expressions. These analytical models have demonstrated reasonable

accuracy for SBVs in the frequency range of 1-50 GHz. However, at high frequencies, the usefulness of these analytical models is limited due to their inability to model high frequency electron transport phenomenon [3-4]. To accurately model high frequency transport phenomena in GaAs SBVs, a Monte Carlo Harmonic-Balance (MCHB) [5] simulator incorporating the Monte Carlo simulator of [6-7] has been developed and offers considerably better precision over results obtained from Harmonic-Balance simulation incorporating equivalent circuit modeling for the diodes [8-9]. Although the MCHB method offers superior accuracy, it is time and CPU intensive and can take from several hours to several weeks to reach a complete multiplier design. To decrease simulation complexity and maintain precision, we have derived a set of analytical design equations with semi-empirical coefficients derived from the MCHB simulator. Since these expressions for device and circuit impedance, efficiency, output power, and d.c. bias are independent of each other and rely solely on nominal device specifications, they allow for co-design from both a device and circuit point of view in a relatively simple, efficient, and accurate manner. Results from the set of design equations are compared to both MCHB simulations and experimental results for a frequency doubler to 200 GHz using a UVA 5T1 varactor diode.

II. Device and Circuit Equations

The following analysis determines a set of equations for the optimal performance of SBV frequency doublers. This set of equations describes the relationship between voltage, current, and power derived from the equivalent circuit model shown in figure 1. Parasitic impedances due to the substrate have been lumped into the linear equivalent circuit embedding impedances and are appropriately accounted for in the calculations of power and efficiency. The following analysis is similar to that of [1-2], but includes the effects of both the nonlinear resistance and capacitance elements.

Given that

$$C(t) \frac{dv(t)}{dt} = i(t) \quad (1)$$

$$\text{and } R(t) = \frac{\rho}{a} (l - w(t)) \quad (2)$$

where ρ is the resistivity of the undepleted active region, a is area of the anode, l is the length of the diode active region, and $w(t)$ is the time dependent depletion width, equations (1) and (2) can be rewritten as

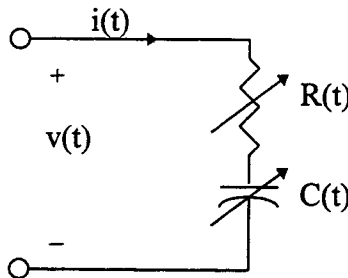


Figure 1 Equivalent varactor circuit model

$$v(t) = \int \frac{1}{C(t)} i(t) dt = \int S(t) i(t) dt \quad (3)$$

$$\text{and } R(t) = \frac{\rho}{a} \left(t - \frac{\epsilon a}{C(t)} \right) = \frac{\rho}{a} [t - \epsilon a S(t)]. \quad (4)$$

Therefore, the time dependent voltage across the diode terminals can be written as

$$v(t) = \frac{\rho^l}{a} i(t) - \epsilon \rho S(t) i(t) + \int S(t) i(t) dt \quad (5)$$

Following the approach of Penfield and Rafuse [1], if an input pump frequency of ω_0 is fed into a harmonic multiplier such as a GaAs SBV, only integer multiples of the form $k\omega_0$ are present. Thus the Fourier representation of the voltage, current, and elastance take the form

$$v(t) = \sum_{k=-\infty}^{\infty} V_k e^{jk\omega_0 t} \quad (6)$$

$$i(t) = \sum_{k=-\infty}^{\infty} I_k e^{jk\omega_0 t} \quad (7)$$

$$S(t) = \sum_{k=-\infty}^{\infty} S_k e^{jk\omega_0 t}. \quad (8)$$

The waveforms $v(t)$, $i(t)$, and $S(t)$ are all real which permits the simplification that

$$\begin{aligned} V_{-k} &= V_k^* \\ I_{-k} &= I_k^* \\ S_{-k} &= S_k^* \end{aligned} \quad (9)$$

where * indicates the complex conjugate. Since the Fourier coefficients are simply phase modified time-averaged values of the time-varying waveforms,

$$V_k = \frac{1}{T_0} \int_{-\frac{T_0}{2}}^{\frac{T_0}{2}} v(t) e^{-\frac{j2\pi kt}{T_0}} dt = \langle v(t) e^{-jk\omega_0 t} \rangle \quad (10)$$

and similarly

$$I_k = \langle i(t) e^{-jk\omega_0 t} \rangle \quad (11)$$

$$S_k = \langle S(t) e^{-jk\omega_0 t} \rangle. \quad (12)$$

Substituting equations (10), (11), and (12) into equation (5) yields

$$V_k = \frac{\rho^l}{a} I_k - \epsilon \rho \langle S(t) i(t) e^{-jk\omega_0 t} \rangle + \frac{1}{jk\omega_0} \langle S(t) i(t) e^{-jk\omega_0 t} \rangle \quad (13)$$

Finally, combining like terms and substituting equations (7) and (8) into equation (13) yields

$$V_k = \frac{\rho^l}{a} I_k + \left(\frac{1}{jk\omega_0} (1 - j\epsilon \rho k \omega_0) \right) \sum_l I_l S_{k-l} \quad (14)$$

where both k and l range from $-\infty$ to $+\infty$. Equation (14) describes the equivalent varactor circuit model in the frequency domain.

Since our analytical model only describes the operation of abrupt junction Schottky barrier diodes, the time-dependent elastance may be expressed as

$$S(t) = \frac{1}{qN_d \epsilon} Q(t) = \frac{1}{C(t)} \quad (15)$$

where N_d is the doping concentration of the active layer of the device. Because the current and charge are related, we can relate equation (15) to the current via

$$i(t) = \frac{dQ(t)}{dt} = qN_d \epsilon \frac{dS(t)}{dt}. \quad (16)$$

In the frequency domain, the current can be expressed as

$$\begin{aligned} \sum_k I_k e^{-jk\omega_0 t} &= qN_d \epsilon \frac{d}{dt} \sum_k S_k e^{jk\omega_0 t} \\ &= qN_d \epsilon (jk\omega_0) \sum_k S_k e^{jk\omega_0 t}. \end{aligned} \quad (17)$$

Since both the summations and phases are identical, we can compare term by term which results in

$$I_k = jk\omega_0 (qN_d \epsilon) S_k. \quad (18)$$

We define the Complex Modulation Ratio, M_k , as the normalized elastance coefficient,

$$M_k = \frac{S_k}{S_{avg}} \quad (19)$$

where $S_{avg} = (S_{max} + S_{min})/2$, S_{max} is defined as the reciprocal of the capacitance at reverse breakdown, and S_{min} is defined as the reciprocal of the capacitance at zero bias. Substituting equations (18) and (19) into equation (14) gives the expression for the harmonic voltage at k

$$V_k = \frac{\rho l}{a} I_k + (qN_d \epsilon) S_{avg}^2 (1 - \epsilon \rho jk\omega_0) \sum_r M_r M_{k-r} \quad (20)$$

The combination of equations (18) and (20) allow us to calculate the device impedance and efficiency. The input impedance at the n^{th} harmonic (where n represents a specific value of k) is given by

$$Z_n = \frac{V_n}{I_n} = \frac{\rho l}{a} + S_{avg} (1 - j\epsilon \rho n\omega_0) \frac{\sum_r M_r M_{n-r}}{jn\omega_0 M_n} \quad (21)$$

If we extract only the real part of equation (21), we arrive at the expression for the resistance of the diode at the n^{th} harmonic

$$R_n = \text{Re}\{Z_n\} = \frac{\rho l}{a} + S_{avg} \left[\frac{A_n}{n\omega_0} - \epsilon \rho B_n \right] \quad (22)$$

where A_n and B_n are real coefficients related to the real parts of the complex modulation ratio summations. The diode reactance at the n^{th} harmonic is given by the imaginary part of equation (21)

$$X_n = \text{Im}\{Z_n\} = S_{avg} \left[\frac{C_n}{n\omega_0} - \epsilon\rho D_n \right] \quad (23)$$

where C_n and D_n are real coefficients related to the imaginary parts of the complex modulation ratio summations. The device efficiency is given by the ratio of the output power at the harmonic of interest to the available input power to the device. Given the complex modulation ratios at each harmonic, each frequency can be considered individually and the expression for the input power at the fundamental frequency ($n = 1$), using equations (18-19) and (22), becomes

$$P_{1,in} = 2(R_1 + R_p)|I_1|^2 = 2(qN_d\epsilon)^2 S_{avg}^2 \omega_0^2 m_1^2 (R_1 + R_p) \quad (24)$$

where $m_n = |M_n|$. R_p is the device parasitic resistance in the substrate and the contact regions of the device as well as the circuit. R_p is always positive and was lumped with the linear embedding circuit impedance at the beginning of this analysis. The second harmonic output power for a doubler is given by a similar expression as equation (24) with the substitution of R_2 for R_1 which results in

$$P_{2,out} = 2(R_2 + R_p)|I_2|^2 = 2(qN_d\epsilon)^2 S_{avg}^2 4\omega_0^2 m_2^2 (R_2 + R_p). \quad (25)$$

Since power is generated at the second harmonic, both R_2 and P_2 are negative for typical doubler designs. As Penfield and Rafuse point out [1], the modulation ratio m_2 is always less than m_1 since the varactor is not an ideal nonlinear capacitor. Also, at frequencies approaching the diode cutoff frequency $m_2 \approx 0$ since the second harmonic current is approximately zero. We approximate m_2 with the following

$$m_2^2 \approx \frac{1}{4} \alpha m_1^2 (1 - \beta f_0 / f_c) \quad \text{for } \beta f_0 \leq f_c \quad \text{where} \quad (26)$$

$$f_c = \frac{1}{2.2 R_{max} C_{max}}$$

where α and β represent the relationship between the modulation ratios m_1 and m_2 and f_c represents the cutoff frequency. R_{max} is the maximum resistance across the diode active region which we define to be $(\rho l / a)$ and C_{max} is defined as the capacitance across the active region at zero bias. The product of R_{max} and C_{max} represents the charging time of the device and the factor of 2.2 accounts for the rise and fall time (the time it takes the device to charge to 90 % and discharge to 10 % of its final value). The inclusion of the cutoff frequency in the modulation ratio aids in the modeling of the effects of diode length and doping on efficiency. The second harmonic power generation efficiency is given by the ratio of the second harmonic output power (25) to the available input power (24) with the substitution of equation (26) for the modulation ratios which becomes

$$\eta = -\frac{P_{2,out}}{P_{in}} = -\alpha \frac{R_2 + R_p}{R_1 + R_p} \left(1 - \beta \frac{f_0}{f_c}\right). \quad (27)$$

As seen, the parasitic resistance contributes to a decrease in efficiency since it serves to increase the magnitude of the of denominator and decrease the magnitude of the numerator in equation (27).

In order to determine the required d.c. bias for optimal performance, we relate the magnitude of the first harmonic voltage to the d.c. bias. Since increased efficiency is observed with increased non-linearity in the capacitance, it is desirable to pump the diode

as close to forward turn-on and breakdown as possible. However, at small incident pump powers, the magnitude of the voltage may not be large enough to reach forward conduction or breakdown. Therefore, since the greatest nonlinear effects in the capacitance are realized when the diode is close to forward turn-on, the d.c. bias should be set approximately equal to the magnitude of the voltage at the first harmonic. The elastance of the diode can be related to the charge by

$$\frac{S - S_{\min}}{S_{\max} - S_{\min}} = \frac{q - Q_{\min}}{Q_{br} - Q_{\min}} \quad (28)$$

where S and q are the unknown elastance and charge at a particular time, respectively, Q_{br} is the charge at reverse breakdown voltage (V_{br}), Q_{\min} is the charge at the minimum applied voltage. The voltage is related to the charge and elastance by

$$V_{Br} = \int_{Q_{\min}}^{Q_{br}} Sdq \quad \text{or}$$

$$Q_{br} - Q_{\min} = \frac{2}{S_{\max} + S_{\min}} V_{br} \quad (29)$$

Since equation (18) can also be written as

$$I_k = j\omega_0 kM_k (Q_{br} - Q_{\min}) \quad (30)$$

we can express the current in terms of the breakdown voltage by substitution of equation (29) into equation (30) which gives the following

$$I_k = j\omega_0 kM_k \frac{2}{S_{\max} + S_{\min}} V_{br} \quad (31)$$

By substituting equation (31) into equation (14) and substituting $|V_{dc}| = |V_1|$ with $n=1$, gives the following expression for the d.c. bias

$$V_{dc} = \frac{1}{(S_{\max} + S_{\min})} \left(\frac{\rho^l}{a} V_{br} \omega_0 \chi + S_{avg} V_{br} (1 - \epsilon \rho \omega_0) \kappa \right) \quad (32)$$

where χ and κ are associated with the complex modulation ratios. Since the MCHB simulator used does not account for breakdown effects, calculated d.c. bias points may bias the device too close to breakdown. Therefore, the general very important guideline applies

$$\left| V_{dc,calculated} \right| \leq \left| \frac{1}{2} V_{br} \right| \quad (33)$$

III. Design Equations and Coefficients for Doublers

In order to utilize the derived set of varactor equations, all the unknown coefficients representing the modulation ratios, which generally are unknown, must be determined. We have solved a global and unified set of coefficients for the analytical equations (22)-(23), (27), and (32) using very accurate numerical simulation results (the MCHB simulator described in [5]). Our analysis considers the case of a GaAs Schottky barrier abrupt junction frequency doubler. We have combined multiple real ratios for each equation into one real coefficient as needed. This results in the following set of design equations for optimal doubler performance

$$R_1 = \frac{\rho^l}{a} + S_{avg} \left(\frac{A}{\omega_0} - \epsilon \rho B \right) \quad (33)$$

$$R_2 = \frac{\rho}{a} + S_{avg} \left(\frac{C}{2\omega_0} - \epsilon \rho D \right) \quad (34)$$

$$X_1 = S_{avg} \left(\frac{E}{\omega_0} - \epsilon \rho F \right) \quad (35)$$

$$X_2 = S_{avg} \left(\frac{G}{2\omega_0} - \epsilon \rho H \right) \quad (36)$$

$$\eta = -\alpha \frac{R_2 + R_p}{R_1 + R_p} \left(1 - \beta \frac{f_0}{f_c} \right) \quad \text{for } f_0 \leq f_c \quad (37)$$

$P_{2,out} = \eta P_{1,in}$, where P_2 is power generated

$$|V_{dc}| = \frac{\rho^l \omega_0}{a(S_{max} + S_{min})} V_{br} \chi + \frac{S_{avg}}{S_{max} + S_{min}} V_{br} (1 - \epsilon \rho \omega_0) \kappa \quad (38)$$

$$|V_1| = |V_{dc}|$$

where A, B, C, D, E, F, G, H, α , β , χ , and κ are the unknown combined modulation ratios. These equations form a complete set of diode and circuit specifications for optimal performance of GaAs SBV frequency doublers. Given a specified diode, the embedding circuit for optimal performance is uniquely determined and the maximum efficiency and output power can be calculated. Also, given a specified circuit, the relationship between the doping and geometry of a diode can be optimally determined for that circuit. For steady state operation and optimal efficiency, the following expressions hold true

$$Z_{1,diode} = Z_{1,circuit}^* \quad \text{and} \quad (39)$$

$$Z_{n,diode} = -Z_{n,circuit} \quad (n \neq 1). \quad (40)$$

Equations (33) - (36) are used to calculate $Z_{n,diode}$.

In order to determine the coefficients, MCHB simulations were run on three different diodes with nominal parameters summarized in table 1 to determine the left hand side of equations (33) - (38). The choice for using three diodes was based on two conditions. First, as can be seen in equations (33) - (38), each equation has two dependent coefficients which would require a minimum of two diode simulations. Second, we wanted to find the coefficients based on an overdetermined set of equations which allows for a minimum mean squared error solution instead of a uniquely determined solution based on two specific diodes. Diodes with doping and length specifications spanning the typical parameters used for high frequency doublers were chosen. For each diode, four different input powers were simulated at both 100 and 275 GHz. The best fit for these overdetermined expressions in equations (33) - (38) was found. For equations (33) - (38), the conventional parameter for resistivity has been used. We can solve for the resistivity through its definition

$$\rho = \frac{1}{q\mu_n N_d} \quad (41)$$

where q is the charge of an electron, N_d is the doping concentration, and we assume μ_n to be the doping dependent constant low-field mobility value of an electron in GaAs. The elastances are calculated as defined earlier. Since l , the length of the diode active region, and a , the area defined by the Schottky contact, are known, we can explicitly solve for the undetermined coefficients. The results from the MCHB simulations are summarized in table 2. The resultant coefficients are summarized in table 3.

Table 1 Nominal Diode Parameters Used to Solve for Unknown Coefficients [10]

Diode	Diode Doping Density (cm ⁻³)	Diode Thickness (μm)	Anode Diameter (μm)	Mobility (cm ² /Vs)	Breakdown Voltage (V)
1	2.0 x 10 ¹⁶	1.5	7.0	6580	31.5
2	3.5 x 10 ¹⁶	1.0	6.3	6400	20
3	4.0 x 10 ¹⁶	0.8	4.7	6340	18

Table 2 Results from Monte Carlo/Harmonic-Balance Simulator for Diodes 1, 2, and 3 (i.e. Right Hand Side of Equations (33) - (38))

Input Frequency (GHz)	P _{1,in} (mW)	Diode	R ₁ device	R ₂ device	X ₁ device	X ₂ device	P _{2,out} (mW)	V ₁ (V)
100	7.5	1	30.3	-27.5	-243.2	-122.6	-2.07	5.29
		2	22.9	-25.0	-213.0	-108.5	-2.92	5.33
		3	35.9	-37.6	-282.3	-147.1	-3.44	5.59
	18.8	1	55.9	-57.3	-273.0	-139.4	-3.58	7.19
		2	39.0	-39.0	-228.3	-116.4	-4.86	7.14
		3	64.1	-58.9	-315.9	-157.6	-5.72	7.95
	29.6	1	81.7	-83.2	-305.9	-153.3	-5.12	8.38
		2	53.4	-51.6	-231.7	-118.9	-5.98	7.84
		3	79.4	-72.7	-320.6	-162.1	-6.92	8.89
	47.0	1	102.1	-99.4	-375.7	-193.4	-5.91	11.77
		2	73.4	-75.7	-272.4	-135.9	-7.57	9.89
		3	96.4	-102.2	-358.7	-181.8	-8.25	11.44
275	7.5	1	17.0	-17.5	-53.6	-30.1	-0.08	1.59
		2	8.6	-11.4	-38.6	-23.0	-0.26	1.47
		3	12.0	-14.7	-69.9	-38.0	-0.49	2.29
	18.8	1	48.1	-48.3	-100.5	-52.9	-0.28	3.04
		2	24.2	-26.4	-57.2	-30.7	-0.74	2.34
		3	35.1	-35.5	-111.5	-63.1	-0.89	3.67
	29.6	1	52.4	-55.9	-143.0	-72.5	-0.38	5.01
		2	35.2	-33.2	-82.2	-47.0	-0.82	3.53
		3	34.9	-33.2	-123.9	-64.2	-1.51	5.48
	47.0	1	37.8	-41.9	-171.6	-88.1	-0.44	8.52
		2	33.8	-30.2	-112.3	-64.1	-1.21	5.98
		3	29.2	-35.6	-158.2	-79.2	-1.89	8.75

Table 3 Resultant Coefficients

$f_{\text{input}} = 100 \text{ GHz}$												
$P_{1,\text{in}}$ mW	A	B	C	D	E	F	G	H	α	β	χ	κ
7.5	0.113	1.681	-0.25	2.727	-0.94	6.623	-1.00	2.519	0.485	5.18	-5.25	0.825
18.8	0.173	-0.08	-0.24	7.02	-1.00	9.025	-0.98	5.149	0.394	7.27	-7.47	1.15
29.6	0.166	-3.93	-0.19	11.35	-0.85	18.01	-0.89	8.452	0.289	5.67	-7.73	1.25
47.0	0.226	-5.13	-0.52	8.966	-0.82	28.65	-0.78	15.73	0.187	4.16	-8.34	1.526

$f_{\text{input}} = 275 \text{ GHz}$												
$P_{1,\text{in}}$ mW	A	B	C	D	E	F	G	H	α	β	χ	κ
7.5	0.027	0.505	-0.07	4.681	-0.55	1.509	-0.62	0.845	0.068	4.26	-0.75	0.308
18.8	0.036	-3.72	-0.02	9.216	-0.58	7.6	-0.74	3.306	0.064	3.78	-0.94	0.458
29.6	0.118	-3.59	0.088	10.96	-0.41	15.56	-0.59	6.977	0.069	4.15	-1.18	0.657
47.0	0.259	-0.09	-0.33	6.727	-0.79	15.50	-0.94	7.374	0.049	4.02	-1.74	1.05

Given the coefficients in table 3 and equations (33) - (38), optimal device and circuit parameters can be quickly calculated for a broad range of input powers and frequencies. Higher harmonic embedding impedances have been shorted.

IV. Design Example

An example of how the design equations and coefficients can be used follows. For this exercise, we wish to compare the results with known experimental results for the UVA 5T1 diode [10]. The nominal device parameters are summarized in table 4. Note that the parameters for this diode are unlike diodes 1, 2, and 3 used for the coefficient extraction.

Table 4 Nominal Diode Parameters for the 5T1 [10]

Diode	Diode Doping Density (cm^{-3})	Diode Thickness (μm)	Anode Diameter (μm)	Mobility (cm^2/Vs)	Breakdown Voltage (V)
5T1	1.0×10^{17}	0.6	4.7	5620	10

Step 1: Choosing a diode length, diode doping, and bias point

First, the diode length is chosen, which for the UVA 5T1 is specified as 0.6 μm . Next, the diode doping density is chosen. Since we are using the UVA 5T1 as an example, the diode doping density, N_d , is $1.0 \times 10^{17} \text{ cm}^{-3}$. Once the doping is chosen, the avalanche breakdown voltage, V_{abr} , should be calculated. The expression for avalanche breakdown voltage is given as

$$V_{\text{abr}} = \frac{1}{2qN_d} \epsilon \xi_{\text{max}}^2 = 10 \text{ V} \quad (42)$$

where ξ_{max} is the maximum electric field obtainable in the diode. An empirical equation we have derived from the measured diode breakdown voltages of actual diodes for ξ_{max} is

$$\xi_{\max} = 1.3 \times 10^{-12} (V \text{cm}^2) \cdot N_d (\text{cm}^{-3}) + 4 \times 10^5 \left(\frac{V}{\text{cm}} \right). \quad (43)$$

For the UVA 5T1, ξ_{\max} is 530 kV/cm which yields a breakdown voltage of 10 V. Because the diode can suffer both avalanche breakdown with and without punch through, the avalanche breakdown voltage (which corresponds to avalanche breakdown without punch through) and the punch through voltage (which determines when punch through occurs and indicates the onset of breakdown) must both be calculated. The smaller of the two voltages should be chosen as the design breakdown voltage, V_{Dbr} , and used in the design equations (33)-(38). The punch through voltage, V_{pt} , is given by

$$V_{\text{pt}} = \frac{1}{2\epsilon} q N d^2 = 25 \text{ V}. \quad (44)$$

Therefore, for this example, the design breakdown voltage, V_{Dbr} , is given by the avalanche breakdown voltage and is 10 V. Once the design breakdown voltage is found, the d.c. bias of the device should be determined from equation (38) and for an input power of 16 mW and an input frequency of 100 GHz, we determine that the magnitude of the d.c. bias should be set at 4.5 V. If the calculated d.c. bias is greater than $V_{\text{Dbr}}/2$ which violates equation (32), the input power could be reduced until equation (32) is satisfied; if the device was punch through limited ($V_{\text{pt}} < V_{\text{br}}$), the length of the device can be increased; or if the device was not punch through limited, the doping can be decreased. If any changes are made to the power, length, or doping, the above process must be repeated until the calculated d.c. bias does not violate equation (32).

Step 2: Determining the optimal embedding impedances, device area, and Q of the diode

Once the length and doping have been determined an anode diameter must be specified which for our example is 4.7 μm . The next step in the solution process is to solve for the resistivity of the device which can be found using equation (41) and is calculated to be 0.01 $\Omega\text{-cm}$. Next, the minimum and maximum elastances must be calculated. These are calculated from the minimum and maximum depletion widths. The depletion width, W , is given by

$$W = \sqrt{\frac{2\epsilon(1+|V|)}{qN_d}} \quad (45)$$

where $|V|$ is the absolute value of the applied voltage (approximately zero for the minimum depletion width corresponding to the minimum elastance and V_{Dbr} for the maximum depletion width corresponding to the maximum elastance). For the UVA 5T1, we calculate that the maximum depletion width, W_{\max} , is 0.40 μm and the minimum depletion width, W_{\min} , is 0.12 μm . Next, the maximum and minimum capacitances are calculated

$$C = \frac{a\epsilon}{W} + \frac{3a\epsilon}{d_{\text{anode}}} \quad (46)$$

where d_{anode} is the device anode diameter, a is the anode area, and W is the depletion width (C_{\min} corresponds to W_{\max} and C_{\max} corresponds to W_{\min}). For the UVA 5T1 whisker contacted diode, the anode area is defined by the anode diameter and is given by

$a = \pi (d_{\text{anode}} / 2)^2$. For the UVA 5T1, we calculate $C_{\text{min}} = 6.3 \text{ fF}$ and $C_{\text{max}} = 17.8 \text{ fF}$. This result yields the following for the minimum and maximum elastances

$$S_{\text{max}} = \frac{1}{C_{\text{min}}} = 1.6 \times 10^{14} \text{ F}^{-1}$$

$$S_{\text{min}} = \frac{1}{C_{\text{max}}} = 5.6 \times 10^{13} \text{ F}^{-1}.$$
(47)

Then, given the coefficients in table 3, the optimal device impedances can be solved for using equations (33) - (36). A comparison of the calculated results and experimental data are presented in table 5. Since the circuit embedding impedances for the experimental data are unknown, results for the impedances of the device and circuit are compared to the accurate MCHB simulator. With the impedances calculated, the Q ($Q_n = X_n / R_n$) for the diode can be calculated. For the UVA 5T1, the calculated value for Q at the first harmonic is approximately 6 ($Q \approx 6$).

Step 3: Determining the output power and second harmonic doubling efficiency

Once the maximum and minimum elastances and the device impedances have been calculated, the second harmonic doubling efficiency can be calculated with equation (37) and the coefficient from Table 3. The cutoff frequency is determined using equation (26) and we find that

$$f_c = \frac{1}{2.2 R_{\text{max}} C_{\text{max}}} = 6.62 \text{ THz.}$$
(48)

Thus, the calculated doubling efficiency for the UVA 5T1 diode is found to be approximately 31 % which results in 5.0 mW of output power at the second harmonic. R_p has been set equal to zero for this example. Hence, for optimal performance at an input frequency of 100 GHz and an input power of 16 mW ($\eta \approx 31 \%$), the embedding circuit impedances should be set to $Z_1 = 30.5 + j 180.5$ and $Z_2 = 25.3 + j 91.1$ and the d.c. bias should be set to -4.5 V. Estimated performance at other frequencies and powers or using different diode parameters can be quickly calculated using table 3.

Table 5 Comparison of Design Equations, Simulated, and Experimental Results for the UVA 5T1 Frequency Doubler at an Input Frequency of 100 GHz

Input Power (mW)	R_1 calc.	R_1 sim.	R_1 exp.	X_1 calc.	X_1 sim.	X_1 exp.	R_2 calc.	R_2 sim.	R_2 exp.
$f_{\text{in}} = 100 \text{ GHz}$									
16	30.5	23.1	NA	-180.5	-174.2	NA	-25.3	-24.5	NA

Input Power (mW)	X_2 calc.	X_2 sim.	X_2 exp.	$P_{2,\text{out}}$ mW calc.	$P_{2,\text{out}}$ mW sim.	$P_{2,\text{out}}$ mW exp.	$ V_{\text{d.c.}} $ calc.	$ V_{\text{d.c.}} $ sim.	$ V_{\text{d.c.}} $ exp.
$f_{\text{in}} = 100 \text{ GHz}$									
16	-91.1	-87.9	NA	5.0	9.0	4.1	4.5	5.0	5.0

Although the calculated impedances cannot be compared to experimental data, they accurately reflect the values predicted by the MCHB simulator and the calculated output power and d.c. bias accurately reflect the experimental data. Many different simulations of various combinations of doping, active layer length, and anode diameter

were performed. The results using the set of design equations yielded consistently accurate results with both MCHB simulation and experimental data where available.

V. Conclusions

A set of design equations for high frequency GaAs SBV frequency doublers has been derived. These equations maintain the simplicity of equivalent circuit modeling while offering superior accuracy. The improvements in accuracy arise from the semi-empirical coefficients contained within the equation set that are derived from a high performance Monte Carlo Harmonic-Balance simulator. These coefficients are found for a variety of powers and two frequencies and can be used to solve for either the nominal diode parameters or the device operating point. Thus, the set of design equations allow for co-design from both a device and circuit standpoint in a simple, efficient, and accurate manner.

Acknowledgments

This research has been sponsored by NSF grant #ECS-9412931. The authors greatly appreciate many important discussions with Tom Crowe, Rob Jones, Greg Tait, and Chris Mann. The authors would also like to recognize the work of Richard Bradley who's dissertation [11] provided an enlightening summary of the Penfield and Rafuse approach in [1].

References

- [1] P. Penfield and R. P. Rafuse, *Varactor Applications*, The M.I.T. Press, Cambridge, Massachusetts, 1962.
- [2] C. B. Burckhardt, "Analysis of Varactor Frequency Multipliers for Arbitrary Capacitance Variation and Drive Level," *The Bell System Technical Journal*, Apr. 1965, pp. 675-692.
- [3] L. F. Horvath, J. R. Jones, S. H. Jones, and G. B. Tait, "Numerical Device/Harmonic-Balance Circuit Analysis of Schottky Barrier Varactors," *Proceedings of the 1995 International Device Research Symposium*, Vol. 1, pp. 259-262, Dec.. 1995.
- [4] J. R. Jones, S. H. Jones, G. B. Tait, "Self-Consistent Physics Based Numerical Device/Harmonic-Balance Circuit Analysis of Heterostructure Barrier and Schottky Barrier Varactors including Thermal Effects," *Proceedings of the Sixth International Symposium of Space Terahertz Technology*, March 1995, p. 423.
- [5] R. E. Lipsey, S. H. Jones, J. R. Jones, T. W. Crowe, L. F. Horvath, U. V. Bhapkar, and R. J. Mattauch, "Monte Carlo Harmonic-Balance and Drift-Diffusion Harmonic-Balance Analyses of 100-600 GHz Schottky Barrier Varactor Frequency Multipliers," Submitted to *IEEE Elec. Dev.*, November 1996.

- [6] U. V. Bhapkar, "Monte Carlo Simulation of GaAs Schottky Diodes for Terahertz Frequencies," Doctoral Dissertation, University of Virginia, August 1995.
- [7] U. V. Bhapkar and R. J. Mattauch, "Monte Carlo Simulation of Terahertz Frequency Schottky Diodes," *Proceedings of the 1995 International Semiconductor Device Research Symposium*, Vol. 1, pp. 263-265, Dec. 1995.
- [8] P. H. Siegel, A. R. Kerr, and W. Hwang, "Topics in the Optimization of Millimeter-Wave Mixers," *NASA Tech. Papers*, No. 2287, Mar. 1984.
- [9] E. L. Kollberg, T. J. Tolmunen, M. A. Frerking, and J. R. East, "Current Saturation in Submillimeter Wave Varactors", *IEEE Trans. on Microwave Theory Tech.*, Vol. 40, No. 5, May 1992, pp. 831-838.
- [10] T. W. Crowe, W. C. B. Peatman, Ru. Zimmermann, and Ra. Zimmermann, "Consideration of Velocity Saturation in the Design of GaAs Varactor Diodes," *IEEE Microwave Guided Waves*, Vol. 3, No. 6, June 1993, pp. 161-163.
- [11] R. F. Bradley, "The Application of Planar Monolithic Technology to Schottky Varactor Millimeter-Wave Frequency Multipliers," Doctoral Dissertation, University of Virginia, 1992.